Anomalous thermal conduction characteristics of phase change composites with single walled carbon nanotube inclusions

Sivasankaran Harish[1], Kei Ishikawa[1], Shohei Chiashi[1], Junichiro Shiomi[1], Shigeo Maruyama[1]

[1]Department of Mechanical Engineering, The University of Tokyo, 7-3-1 Hongo, Bunkyo-ku, Tokyo 113-8656, Japan.

We report large contrasts in the thermal conductivity enhancement of phase change alkanes in liquid and solid state with single walled carbon nanotube (SWCNT) inclusions. Well characterized SWCNTs grown by alcohol catalytic chemical vapor deposition method were dispersed in the phase change alkane using sodium deoxycholate (DOC) surfactant. Thermal conductivity measurements in solid and liquid state were carried out using a transient hot wire technique for different SWCNT loadings. The thermal conductivity contrast between liquid and solid state was found to increase with increasing SWCNT loadings. Similar phase dependent thermal conductivity contrast was observed when were used as the inclusions. The thermal conductivity contrast was more pronounced in the presence of SWCNTs compared to the presence of exfoliated graphite nanoplatelets.

Thermal energy storages using phase change materials, substances which charge/discharge energy by melting/solidification, are often employed in waste heat recovery, solar energy storage, etc.[1, 2] The latent heat energy storages requires high thermal conductivity of the phase change materials, because low thermal conductivity hinders the rate of energy storage and release of the phase change materials.[1] Advancements in the field of nanotechnology have led to the development of the new way of improving the thermal conductivity of phase change materials by seeding nano materials of different shape.[3,4] These phase change materials with nano inclusions are already frequently used for latent heat storage applications. However, attempts to improve

the thermal conductivity of the phase change materials with nano inclusions have been very limited and are still in developing stage.[5-8] Recently, Zheng et al.[9] reported a thermal conductivity contrast between liquid and solid state by a factor of 3.2 in *n*-hexadecane with 1 vol% loading of graphite inclusion during first order phase change process.

In this paper, we investigate the thermal conductivity contrasts of phase change alkane *n*-octadecane with one dimensional SWCNT nano inclusions and compare its performance with exfoliated graphite nanoplatelets (GnP). A contrast ratio of 2.9 is achieved at a SWCNT loading of 0.25 wt%. GnP inclusions achieved a lesser contrast ratio of 2.1 at a loading of 0.45 wt%. The present experiments introduced an efficient way to manipulate the thermal conductivity of nano composites using one dimensional nano material inclusion by effectively controlling the heat transport path simply via temperature regulation.

The SWCNTs used in this study were synthesized by the alcohol catalytic chemical vapour deposition (ACCVD) technique using cobalt and iron bi-metallic catalysts supported on zeolite particles (HSZ-390HUA).[10] Ethanol vapour was employed as the carbon feedstock, and the reaction temperature was maintained at 800°C. After CVD, zeolite particles were removed by dissolving in sodium hydride solution.

A typical transmission electron microscopy (TEM) image of the SWCNTs synthesized from ethanol feedstock is shown in Figure 1(a). Neither amorphous carbon nor metal particle impurities are observed in the TEM visualization. Raman spectra obtained from the SWCNT sample is shown in Figure 1(b). Radial breathing mode (RBM) peaks seen in the low-frequency region (100–400 cm^{-1}) are unique to SWCNTs and are not observed in other carbon allotropes. The G-band observed at 1594 cm^{-1} is a characteristic feature of sp^2-bonded graphitic carbon, and

corresponds to in-plane vibrations of the carbon atoms. The D-band found near 1350 cm^{-1} arises from defects in the tube walls or from amorphous carbon impurities. The suppressed D-band intensity in the Raman spectra indicates that defects in the tube walls and the amorphous carbon impurities were less. Thermogravimetric analysis (TGA) of the SWCNTs shown in figure 1(c) revealed that the SWCNTs uniformly burnt at a temperature of 600^0 C. Since amorphous carbon decomposes at around 300 ^oC – 500 ^oC, which is lower than the decomposition temperature of SWCNTs, the TGA result proved absence of amorphous carbon impurities.[11] The TEM investigation, the Raman spectra, and the TGA analysis showed the absence of structural defects or impurities such as metals or amorphous carbons in the ACCVD grown SWCNTs.

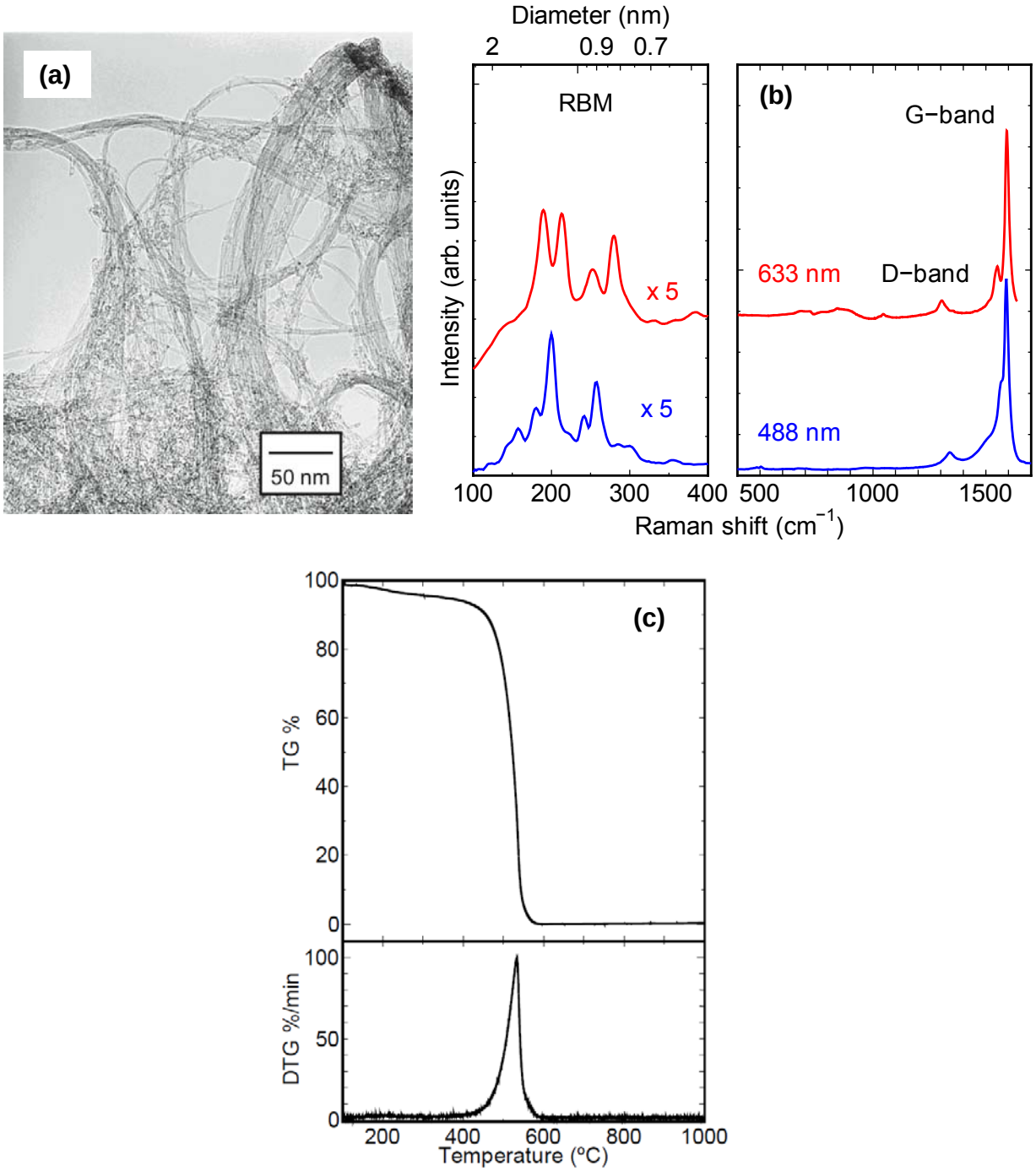

Figure 1: (a) Typical TEM image of SWCNTs taken at an acceleration voltage of 120 kV. (b) Resonance Raman spectra of SWCNTs taken at 488 nm and 633 nm laser excitation. The Graphite-like band (G-band), the defect induced peak (D-band) and the radial breathing mode (RBM) peaks are shown with an added diameter scale. The diameter (d) was calculated using the equation $\omega_{RBM} = 217.8/d + 15.7$.[12] (c) Thermogravimetric analysis of SWCNTs performed at a heating rate of 0.5 ^{o}C/min.

The synthesized SWCNTs were dispersed in *n*-Octadecane (*n*-$C_{18}H_{38}$) [99.5% purity purchased from Sigma Aldrich] whose freezing point is close to 300K, using 1 wt% of the surfactant sodium deoxycholate (DOC), which is proven to create stable dispersions based on our previous studies.[13,14] The dispersions were subjected to sonication using an ultrasonic processor (Hielscher GmbH, UP-400S with H3/Micro Tip 3) for 2 hours at a power flux level of 360 W/cm^2 (80% amplification). The exfoliated graphite nanoplatelets (GnP) [Purchased from XG Sciences, Grade-M, USA] were also dispersed in the similar manner.

The thermal conductivity measurements were carried out using the transient hot wire (THW) technique which is described elsewhere.[15] We made use of a platinum (Pt) hot wire of length 50.0 mm and 25.4 μm diameter with an electrically insulating isonel coating of 2.0 μm. A detailed uncertainty analysis of the experimental setup shows that the random uncertainties of experiments were ± 0.5% and the systematic uncertainties (i.e due to the inaccuracies in the hotwire length and fitting error to calculate the slope) ± 2 %.

The thermal conductivity measurement results of the *n*-Octadecane (*n*-$C_{18}H_{38}$) with loadings of SWCNT inclusions and temperature as parameters showed that the thermal conductivity contrast increased with higher SWCNT loading, as shown in figure 2(a) and 2(b). The present experimental values of the pristine *n*-Octadecane (*n*-$C_{18}H_{38}$) thermal conductivity were consistent with the literature values.[16] With the inclusion of SWCNTs, a limited improvement in thermal conductivity was noticed in liquid state while a larger improvement in the solid state was noticed with increasing SWCNT loading. Maximum thermal conductivity contrast ratio of 2.9 was reached at much lower SWCNT loading of 0.25 wt% (~ 0.15 vol%) compared with the graphite inclusion in n-hexadecane.[9]

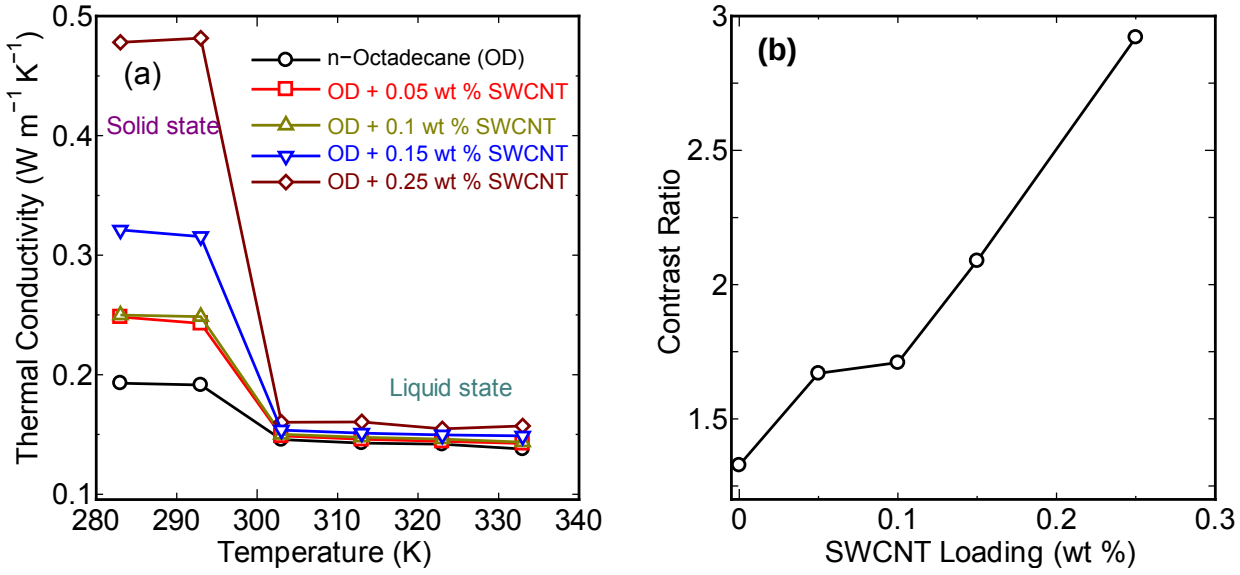

Figure 2: (a) Thermal conductivity of *n*-Octadecane as a function of temperature for varying SWCNT loadings. The freezing point of the *n*-Octadecane is approximately 300 K. A sharp increase in thermal conductivity in the solid state is seen. (b) Contrast ratio (solid state thermal conductivity to liquid state thermal conductivity) as a function of SWCNT loading. Maximum contrast ratio of 2.9 is achieved at a SWCNT loading of 0.25 wt%.

We also estimated the effective thermal conductivity of the composites using classical theoretical models. Assuming the SWCNTs as randomly oriented rigid ellipsoidal structures and taking into account the effect of thermal boundary resistance (TBR), we calculated the effective thermal conductivity enhancement using Maxwell-Garnett type effective medium theory (EMT) as reported in Nan et al.[17] and a modified Yamada – Ota empirical model as reported in Zheng and Hong[18,19] (See supporting information). For the present model calculations, we made use of the fluid state thermal conductivity of 0.143 W m^{-1} K^{-1}, [16] solid state thermal conductivity of 0.193

W m^{-1} K^{-1},[16] SWCNT thermal conductivity of 1000 $Wm^{-1}K^{-1}$,[20] and SWCNT aspect ratio (L/d) of 500 based on our atomic force microscopy (AFM) measurements[14]. The thermal boundary resistance (TBR) was taken of the order of 10^{-8} m^2 K W^{-1} and assumed to be constant over the range of temperature tested.[21,22] Length distribution of SWCNTs post sonication in our present experiments based on AFM measurements was in the range of 100 - 600 nm[14]. In these models the SWCNTs were assumed as rigid rods and the influence of the waviness of the SWCNTs was neglected.

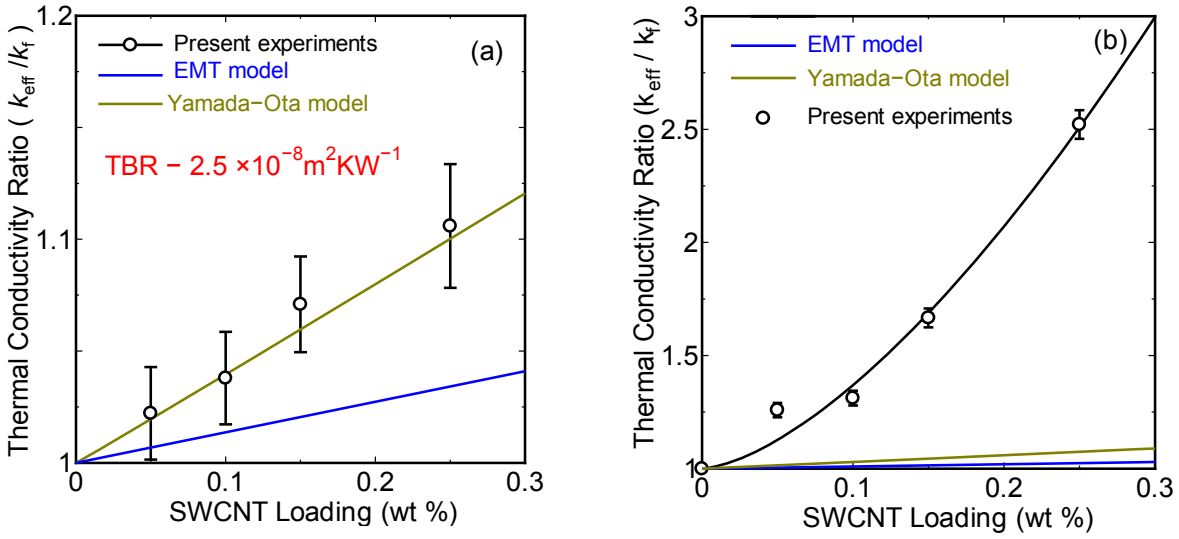

Figure 3: (a) Thermal conductivity enhancement in liquid state as a function of SWCNT loading. Modified Yamada-Ota model predict the present experimental results with a TBR of 2.5 x 10^{-8} m^2KW^{-1}. EMT model prediction for the same TBR in the liquid state is marginally lesser compared to modified Yamada-Ota model. (b) Thermal conductivity enhancement in solid state as a function of SWCNT loading. The theoretical models fail to predict the enhancement in solid state as the influence of aggregation during first order phase transition is not included in the models. The experimental results were fitted with a power law equation of form $A\phi_w^b$ where A

and *b* were fitting constants and ϕ_w is the SWCNT weight fraction. The fit parameters were 12.6 and 1.53 for *A* and *b* respectively.

Figure 3(a) and 3(b) show the effective thermal conductivity enhancement in liquid state and solid state along with the predictions of theoretical models. In the liquid state, the thermal conductivity enhancement was in a linear fashion with respect to the SWCNT loading as shown in figure 3(a). The modified Yamada-Ota model can predict the experimental results with a reasonable TBR of 2.5×10^{-8} m^2KW^{-1} (Thermal boundary conductance of 40 MW/m^2K) while the EMT model predicted a marginally lower enhancement with the same TBR. However, both theoretical models fail to explain the high thermal conductivity enhancement noticed in the solid state. Besides, the enhancement in the solid state remains marginally non-linear with respect to SWCNT loading while in the liquid state a linear enhancement is noticed.

Higher thermal conductivity enhancement observed in the solid state possibly indicates the formation of quasi two-dimensional cellular structure during the phase transition process. It may be possible that transition from 3D percolated network of carbon nanotubes to 2D percolated network promoted the interaction among SWCNTs thus increasing the heat transport path in a non-linear way which is in consistent with the simulation results reported in Ref.23. Besides, recent simulation study suggest that alkane molecules surrounding the nanotubes when frozen to solid state exhibit a tendency to form lamellar layers along nanotube axis and exhibit two-dimensional structural ordering in planes perpendicular to the nanotube axis which is similar to the crystalline polymers[24]. Hence it may be possible that the two dimensional structural ordering of SWCNTs and SWCNT induced molecular alignment during phase transition can lead to the high thermal conductivity enhancement of the nano composite in frozen state [25, 26].

The process remained reversible for the subsequent cycles as shown in figure 4. When the nano composite was reheated back to the same liquid state, the original 3D networks of the dispersions might recover or molecular disordering occurs which disrupts the crystalline structure of the alkane. Hence, the liquid state thermal conductivity enhancement remains lower than the solid state thermal conductivity.

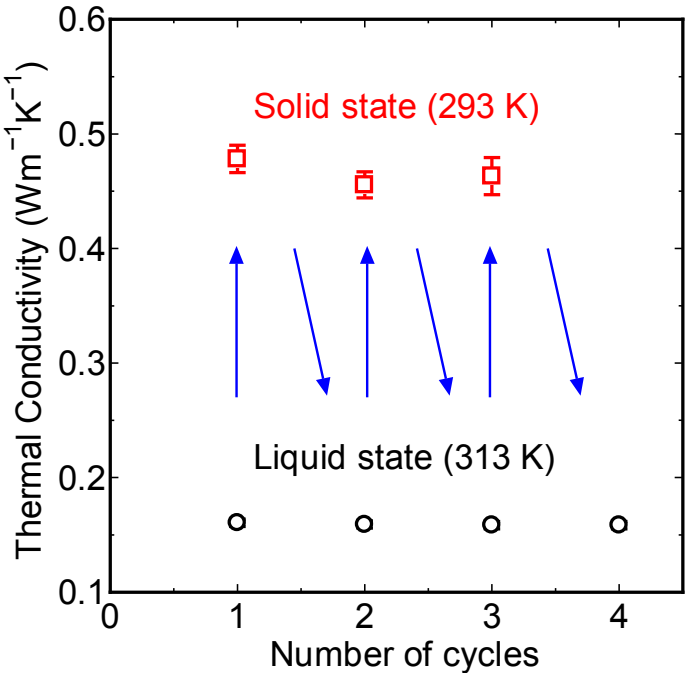

Figure 4: Recycling behaviour of thermal conductivity during successive phase transition cycles at SWCNT loading of 0.25 wt%. Arrows indicate the sequence of cycles.

We performed additional experiments with commercially available exfoliated graphite nanoplatelets (GnP, 4-10 nm thickness) as inclusions in *n*-octadecane. Similar anomalous thermal conductivity contrasts were also observed in the presence of two dimensional inclusions which is shown in figure 5. The present experimental results with GnP were marginally lower

than the results with graphite suspensions reported in Ref. 9. A contrast ratio of approximately 2.1 was achieved at a GnP loading of 0.45 wt%.

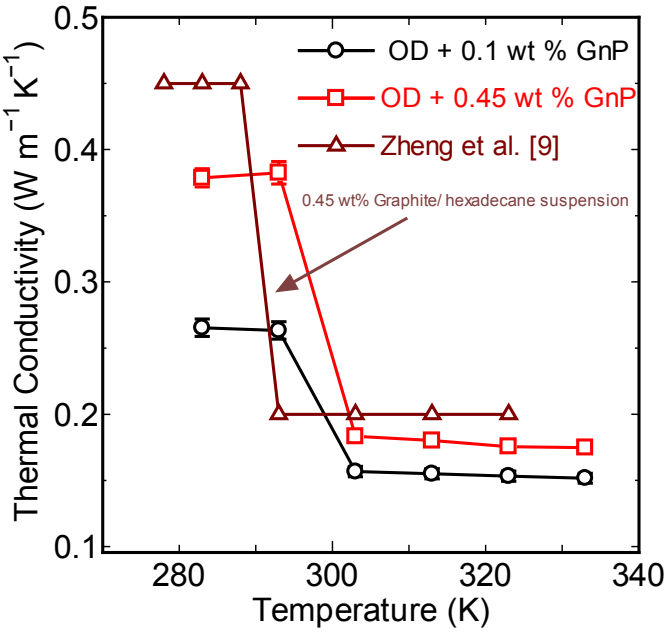

Figure 5: Comparison of the GnP (graphene nanoplatelets) dissolved into OD (*n*-octadecane) with different loadings and the graphite dissolved into hexadecane reported by Zheng et al. [9]. Sharp increase in thermal conductivity is noticed during freezing with two dimensional graphite nanoplatelets as inclusions.

The thermal conductivity contrast is noticed irrespective of whether the inclusion is SWCNTs, or GnPs. The present experimental results show that much higher thermal conductivity contrast was achieved with lower loading of SWCNTs as compared to the GnP. The SWCNT showed contrast ratio of 2.9 with 0.25 wt% loading, whereas the GnP showed a contrast ratio of 2.1 with 0.45 wt% loading. This may possibly due to the ability of the SWCNTs to induce the formation of stronger crystalline networks than GnPs[25,27]. Besides, the superior performance of SWCNTs over GnPs may possibly due to the tendency of alkane chain to get adsorbed on to the CNT surface

and align themselves parallel to the axis of the CNT, while the alkane chains show multiple orientations on the GnP surface.[27]

In the present study, we have limited our measurements to low SWCNT loadings because of the difficulty in achieving good stability at higher loading of SWCNT with the current surfactant assisted dispersion method. However, with improved dispersion techniques there is a potential for higher thermal conductivity contrast and higher thermal conductivity enhancement in phase change materials with nano inclusions of SWCNTs.

In summary, we report contrasting thermal conductivity enhancement in phase change alkane with one dimensional SWCNT nano inclusions and compare its performance with two dimensional exfoliated GnP nano inclusions. The solid/liquid thermal conductivity contrast was found to increase with higher SWCNT loadings. Classical theoretical models fail to explain the measured contrasting thermal conductivity improvements. SWCNT inclusions perform better than the GnP inclusions during the phase transition. Further research need to focus on the development of theoretical models to explain such contrasting behaviour.

This work was financially supported in part by Grant-in-Aid for Scientific Research (22226006 and 23760179) and the "Global Center of Excellence for Mechanical Systems Innovation" (GMSI). SH was financially supported by the Japanese Government Monbukagakusho (MEXT) Scholarship, A part of this work was conducted in the Research Hub for Advanced Nano Characterization, the University of Tokyo, supported by the Ministry of Education, Culture, Sports, Science and Technology, Japan.

[1] H. Inaba, Int. J. Therm. Sci. **39** (9-11), 991 (2000).

[2] L. W. Fan and J. M. Khodadadi, Renew. Sustain. Energy Rev. **15** (1), 24 (2011).

[3] L. Godson, B. Raja, D. M. Lal, and S. Wongwises, Renew. Sustain. Energy Rev. **14** (2), 629 (2010).

[4] J. Fan and L. Q. Wang, J. Heat Transfer **133** (4) (2011).

[5] A. Sari and A. Karaipekli, App. Therm. Eng. **27** (8-9), 1271 (2007).

[6] Y. D. Liu, Y. G. Zhou, M. W. Tong, and X. S. Zhou, Microfluid. Nanofluid. **7** (4), 579 (2009).

[7] C. J. Ho and J. Y. Gao, Int. Comm. Heat Mass Transfer **36** (5), 467 (2009).

[8] J. F. Wang, H. Q. Xie, and Z. Xin, Thermochim. Acta **488** (1-2), 39 (2009).

[9] R. Zheng, J. Gao, J. Wang, and G. Chen, Nat. Commun. **2**, 289 (2011).

[10] S. Maruyama, R. Kojima, Y. Miyauchi, S. Chiashi, and M. Kohno, Chem. Phys. Lett. **360** (3-4), 229 (2002).

[11] Y. Murakami, Y. Miyauchi, S. Chiashi, and S. Maruyama, Chem. Phys. Lett. **374** (1-2), 53 (2003).

[12] P. T. Araujo, S. K. Doorn, S. Kilina, S. Tretiak, E. Einarsson, S. Maruyama, H. Chacham, M. A. Pimenta, and A. Jorio, Phys. Rev. Lett. **98** (6), 067401-1 (2007).

[13] S. Harish, K. Ishikawa, E. Einarsson, S. Aikawa, T. Inoue, P. Zhao, M. Watanabe, S. Chiashi, J. Shiomi, and S. Maruyama, Mater. Express **2** (3), 213 (2012).

[14] S. Harish, K. Ishikawa, E. Einarsson, S. Aikawa, S. Chiashi, J. Shiomi, and S. Maruyama, Int. J. Heat Mass Transfer **55** (13-14), 3885 (2012).

[15] Y. Nagasaka and A. Nagashima, J. Phys. E Sci. Instrum. **14** (12), 1435 (1981).

[16] R. W. Powell, A. R. Challoner, and W.M F. Seyer, Ind. Eng. Chem. Res. **53** (7), 581 (1961).

[17] Ce-Wen Nan, R. Birringer, David R. Clarke, and H. Gleiter, J. Appl. Phys. **81** (10), 6692 (1997).

[18] E. Yamada and T. Ota, Heat Mass Transfer **13** (1-2), 27 (1980).

[19] Y. Z. Zheng and H. P. Hong, J. Thermophys. Heat Transfer **21** (3), 658 (2007).

[20] S. Maruyama, Microscale Therm. Eng. **7** (1), 41 (2003).

[21] S. T. Huxtable, D. G. Cahill, S. Shenogin, L. P. Xue, R. Ozisik, P. Barone, M. Usrey, M. S. Strano, G. Siddons, M. Shim, and P. Keblinski, Nat. Mater. **2** (11), 731 (2003).

[22] S. D. Kang, S. C. Lim, E. S. Lee, Y. W. Cho, Y. H. Kim, H. K. Lyeo, and Y. H. Lee, ACS Nano **6** (5), 3853 (2012).

[23] A. N. Volkov and L. V. Zhigilei, Phys. Rev. Lett. **104** (21), 215902 (2010).

[24] C.-Y. Wei, Phys. Rev. B **76** (13), 134104 (2007).

[25] J. S. Yang, C. L. Yang, M. S. Wang, B. D. Chen, and X. G. Ma, Phys. Chem. Chem. Phys. **13** (34), 15476 (2011).

[26] H. Babei, P. Keblinski, and J. M. Khodadadi, Int. J. Heat Mass Transfer **58** (1-2), 209 (2012).

[27] J. Z. Xu, T. Chen, C. L. Yang, Z. M. Li, Y. M. Mao, B. Q. Zeng, and B. S. Hsiao, Macromolecules **43** (11), 5000 (2010).

Supporting Information

Anomalous thermal conduction characteristics of phase change composites with single walled carbon nanotube inclusions

Sivasankaran Harish[1], Kei Ishikawa[1], Shohei Chiashi[1], Junichiro Shiomi[1], Shigeo Maruyama[1]

[1]Department of Mechanical Engineering, The University of Tokyo, 7-3-1 Hongo, Bunkyo-ku, Tokyo 113-8656, Japan.

Empirical equation for thermal conductivity enhancement

The EMT model is shown in equation (1):[1]

$$\frac{k_{eff}}{k_b} = 1 + \frac{\phi L}{d} \frac{(k_{SWCNT}/k_b)}{\frac{L}{d} + \frac{2a_k}{d}\frac{k_{SWCNT}}{k_b}} \tag{1}$$

Here L and d are the nanotube length and diameter respectively. k_b is the base matrix thermal conductivity, k_{SWCNT} is the thermal conductivity of SWCNT, k_{eff} is the effective thermal conductivity, ϕ is the SWCNT volume fraction, a_k is the Kapitza radius, which is defined as the product of thermal boundary resistance (TBR) and the thermal conductivity of the base matrix ($a_k = TBR \times k_b$). The model proposed by Zheng and Hong incorporating the TBR in the original Yamada–Ota model is shown in equation (2)[2,3]

$$\frac{k_{eff}}{k_b} = \frac{(k_x/k_b) + \alpha - \alpha\phi[1-(k_x/k_b)]}{(k_x/k_b) + \alpha + \phi[1-(k_x/k_b)]} \tag{2}$$

where $k_x = \frac{k_{SWCNT}}{1 + \left(\frac{2k_{SWCNT}(TBR)}{L}\right)}$ and $\alpha = 2\phi^{0.2}\left(\frac{L}{d}\right)$. The notations in equation (2) are the same as in equation (1).

1 Ce-Wen Nan, R. Birringer, David R. Clarke, and H. Gleiter, J. Appl. Phys. **81** (10), 6692 (1997).

2 E. Yamada and T. Ota, Heat Mass Transfer **13** (1-2), 27 (1980).

3 Y. Z. Zheng and H. P. Hong, J. Thermophys. Heat Transfer **21** (3), 658 (2007).